

Research Article

Development of a Coupled EnergyPlus-MATLAB Simulation Based on LSTM for Predictive Control of HVAC System

YiLin Cong , LiTong Hou , YiCheng Wu , and YongZhi Ma 

School of Electromechanic Engineering, Qingdao University, Qingdao 266071, Shandong, China

Correspondence should be addressed to YongZhi Ma; hiking@126.com

Received 27 April 2022; Revised 28 August 2022; Accepted 13 October 2022; Published 26 October 2022

Academic Editor: Kauko Leiviskä

Copyright © 2022 YiLin Cong et al. This is an open access article distributed under the Creative Commons Attribution License, which permits unrestricted use, distribution, and reproduction in any medium, provided the original work is properly cited.

To avoid unnecessary energy waste due to the single temperature setpoints of the heating, ventilation, and air conditioning (HVAC) system during the seasonal variation period, this study proposed a long-short-term memory (LSTM) neural network to predict and control the temperature setpoint. The thermal comfort, cooling rate, and heating rate were predicted with outdoor environment parameters and occupant count. A large scale of operation data was collected from the EnergyPlus simulation, which was previously developed based on the characteristics of a real case study house. Different kinds of input characteristics were offered to test the stable use of LSTM and other artificial neural networks. This paper discusses the development of a Matlab EnergyPlus co-simulation to predict and control the temperature setpoints of a variable air volume system, especially the relationship between temperature setpoint and energy consumption. The simulation results indicate the advantages of the LSTM prediction of energy consumption and the potential for energy saving with predictive control.

1. Introduction

Building energy consumption accounts for about 40% of the global total energy consumption and is expected to reach about 50% by 2030 [1, 2]. Recent research proved that dynamic temperature control can be employed in HVAC systems according to building characteristics and outdoor environment to avoid unnecessary energy waste [3, 4], especially in seasonal variation period [5].

Dynamic control of HVAC system temperature relies on its model and simulation. Data-driven, physics-based, and grey box modelling techniques are used to complete the model of the HVAC system [6]. Compared to other control objects, the control of HVAC has unique challenges, including nonlinear dynamics, time-varying system dynamics and setpoints, time-varying disturbances, interacting, and at times conflicting control loops [7]. To simplify the HVAC model, linearized sampled data were used with a regression analysis method, such as least absolute shrinkage and selection operator [8]. Economic objective functions are offered with predictive control of HVAC for load transfer and cost saving [9].

Cosimulation is often used to provide advanced control strategies for building energy management systems. Many of the previous studies used energy simulators such as TRNSYS, EnergyPlus, and Matlab/Simulink to simulate the HVAC operating conditions. Peng et al. [10] used Matlab and EnergyPlus co-simulation to study the PID control of thermal comfort in four typical kinds of climates, depending on the occupancy rate of buildings. Lapusan et al. [11] studied an equivalent thermal multiroom model in Simscape, a toolbox of Matlab. The main aim of this paper is to build a simulation tool based on physical models. Avoiding incompatibility problems comes from doing the modelling in the Simulink environment. To utilize an artificial neural network (ANN) to simulate the model predictive control of the HVAC system, Venkatesan et al. [12] established a heat flow model and equivalent thermal model from EnergyPlus. Alibabaei et al. [13] used a TRNSYS-Matlab cosimulator with an advance control strategy to study the efficiency of different strategy models. Narayanan et al. [14] developed a TRNSYS and Matlab co-simulation framework, which was used to implement MPC and optimization algorithms in a standard single-family house. Wang et al. [15] utilized a

reinforcement learning controller in Matlab to control EnergyPlus depending on building controls virtual test bed (BCVTB). Rosato et al. [16] used experiments to test the accuracy of TRNSYS and Matlab co-simulation model. The correlation coefficients of supply air temperature and open percentage of different valves were above 0.95. Homod et al. [17] developed a co-simulation framework between Matlab and ANSYS to verify the accuracy of the HVAC model. The correlation coefficient of indoor temperature was 0.9897, and the coefficient of the vernacular predicted mean value (PMV) is 0.839.

The prediction errors between different articles were difficult to compare because of different input features. The input features of LSTM predictions lacked past energy consumption, and the RMSE of it reached 618.40 [18]. Some used energy-normalized RMSE as a criterion for prediction accuracy, and the RMSE of it reached 0.13 [19]. Mtibaa et al. used LSTM neural network to predict indoor temperature, which showed that the LSTM models outperform multilayer perceptron models by reducing the prediction error by 50% [20]. To control the thermal comfort with smart WIFI, Huang et al. compared back-propagation (BP) neural network with LSTM and encoder-decoder LSTM about thermostat setting. The LSTM control reduced the range of heating and cooling by 14.3% significantly [21].

Thermal comfort is not only the limit of temperature setpoints but also the evaluation standard of temperature control effect. Baldi et al. [22] developed a self-tuning load management program with smart zoning to reduce energy by 4% and improve thermal comfort by 8% in an actual EnergyPlus model. De Dear et al. [23] reviewed the research progress on adaptive thermal comfort and some outstanding problems since 1998, such as the intersection of thermal comfort temperature in the conventional comfort model and adaptive comfort model based on RP-884 (actual observation database). Alfano et al. [24] summarized the calculation methods of thermal comfort software on the APP market and the problems needing attention in the process of PMV calculation. Cao et al. [25] reviewed the research related to dynamic thermal comfort, aiming to explain the development, prospects, and necessity of dynamic thermal comfort research. Somu et al. [26] used transfer learning and a comprehensive thermal comfort evaluation index to solve the lack of thermal comfort samples. Korkas et al. [27] guaranteed the independence of microgrid with supervisory

strategy to improve the thermal comfort when energy storage and renewable energy sources are used.

In this paper, environmental parameters are used to set thermostat of HVAC based on LSTM prediction in a co-simulation platform. The paper consists of 4 sections. In Section 2, the Matlab and EnergyPlus co-simulation platforms are described. The process models of simulation and an overview of the principle of LSTM are also described, especially focusing on the input and output parameters of the prediction model. In Section 3, we will provide results and a discussion about the simulation. In Section 4, the conclusion is provided.

2. Materials and Methods

2.1. EnergyPlus Simulation. The simulation location is set at 20.03°N, 110.35°E, which belongs to the tropical monsoon marine climate. The run period of the control simulation is from March 1st to April 30th (the latter spring and early cooling period [3]). The run period of the simulation without control is from January 1st to December 31st for comparison. The HVAC system in this paper is a variable air volume system with reheat, including chiller, cooling water coil, heating water coil, variable pump, variable fan, boiler, and cooling tower. The floor area is 98 m², and the building height is 3 m. Tables 1 and 2 and Figure 1 show other parameters of the EnergyPlus building model.

The energy consumption of the water chilling unit in the EnergyPlus simulation is calculated by the chilled water outlet temperature and inlet water temperature of the compressor at the rated conditions. The formula is built by experimental data, and the data from manufacturers are based on the least-squares method.

2.2. Thermal Comfort. The thermal comfort model plays a significant role in LSTM neural network prediction. PMV is used as a widely used index in evaluating users' thermal comfort. According to the ISO-7730 standard, the factors affecting PMV include indoor air temperature, mean radiation temperature, relative humidity, metabolic rate, mechanical work, clothing isolation value, and clothing surface temperature [28]. The following PMV calculation formula works well except under high relative humidity:

$$\begin{aligned}
 PMV &= [0.303 \cdot \exp(-0.036 \cdot M) + 0.028] \cdot \\
 &\left\{ \begin{aligned} &(M - W_p) - 3.05 \cdot 10^{-3} \cdot [5733 - 6.99 \cdot (M - W_p) - p_a] - 0.42 \cdot [(M - W_p) - 58.15] \\ &- 1.7 \cdot 10^{-5} \cdot M \cdot (5867 - p_a) - 0.0014 \cdot M \cdot (34 - t_a) - 3.96 \cdot 10^{-8} \cdot f_{cl} \cdot [(T_{cl} + 273)^4 - (\bar{T}_r + 273)^4] - f_{cl} \cdot h_c \cdot (T_{cl} - T_a) \end{aligned} \right\}, \\
 T_{cl} &= 35.7 - 0.028 \cdot (M - W_p) - I_{cl} \cdot \left\{ 3.96 \cdot 10^{-8} \cdot f_{cl} \cdot [(T_{cl} + 273)^4 - (\bar{T}_r + 273)^4] + f_{cl} \cdot h_c \cdot (T_{cl} - T_a) \right\}, \\
 h_c &= \begin{cases} 2.38 \cdot |T_{cl} - T_a|^{0.25} & \text{for } 2.38 \cdot |T_{cl} - T_a|^{0.25} > 12.1 \cdot \sqrt{v_{ar}} \\ 12.1 \cdot \sqrt{v_{ar}} & \text{for } 2.38 \cdot |T_{cl} - T_a|^{0.25} < 12.1 \cdot \sqrt{v_{ar}} \end{cases}, f_{cl} = \begin{cases} 1.00 + 1.290 I_{cl} & \text{for } I_{cl} \leq 0.078 m^2 \cdot \frac{K}{W_p} \\ 1.05 + 0.645 I_{cl} & \text{for } I_{cl} > 0.078 m^2 \cdot \frac{K}{W_p} \end{cases}.
 \end{aligned} \tag{1}$$

TABLE 1: Thermal physical parameters of the building envelope.

Construction	Thickness (mm)	Heat transfer coefficient W/(m ² ·K)
Exterior wall	265	0.79
Roof	250	0.77
Floor	220	1.32
Interior wall	240	1.19

TABLE 2: Factors of occupancy, lighting, and electrical equipment on work day.

	Time																							
	1:00	2:00	3:00	4:00	5:00	6:00	7:00	8:00	9:00	10:00	11:00	12:00	13:00	14:00	15:00	16:00	17:00	18:00	19:00	20:00	21:00	22:00	23:00	0:00
People	0	0	0	0	0	0	0.1	0.2	0.8	0.8	0.8	0.8	0.8	0.8	0.8	0.8	0.8	0.8	0.8	0.8	0.1	0	0	0
Lights	0	0	0	0	0	0.1	0.1	0.3	0.9	0.9	0.9	0.9	0.9	0.9	0.9	0.9	0.9	0.7	0.5	0.5	0.3	0.3	0	0
Equip	0.4	0.4	0.4	0.4	0.4	0.4	0.4	0.4	0.9	0.9	0.9	0.9	0.8	0.9	0.9	0.9	0.9	0.8	0.6	0.6	0.5	0.5	0.4	0.4

In order to simplify the model, mechanical work is set to zero. The above formulas are used to calculate thermal comfort during EnergyPlus simulation, which has limitations. When using neural network to predict the thermal comfort of occupancy, it can be modified appropriately. It is difficult to measure clothing surface temperature and metabolic rate in practical applications. Therefore, the former features are not used as the input to the prediction of the LSTM neural network.

2.3. LSTM Prediction. To fit the diffusion or explosion of the gradient with recurrent neural network (RNN), LSTM was proposed [29]. LSTM includes input gate, output gate, forget gate, cell gate as shown in Figure 2. The Adam optimizer is chosen. It has strong adaptability to training parameters as the default optimizer in many application scenarios. The gradient threshold is 1, the initial learning rate is 0.005, the learning rate drop period rate is 125, and the drop factor is 0.2. After testing and verification, the above parameters can control the training time and accuracy within a relatively reasonable range. In order to strengthen the learning ability of the LSTM neural network and avoid overfitting or other problems caused by too many hidden units, the influence of different numbers of hidden units about the error of the test set is tested, and the prediction is better when 48 hidden units are tested.

$$\begin{aligned}
\text{forget gate: } f_t &= \sigma(W_f x_t + U_f h_{t-1} + b_f), \\
\text{input gate: } i_t &= \sigma(W_i x_t + U_i h_{t-1} + b_i), \\
\text{cell state: } c'_t &= \text{Tanh}(W_c x_t + U_c h_{t-1}), \\
c_t &= f_t c_{t-1} + i_t c'_t, \\
\text{output state: } o_t &= \sigma(W_o x_t + U_o h_{t-1} + b_o), \\
h_t &= o_t \text{Tanh}(c_t).
\end{aligned} \tag{2}$$

The prediction error of the LSTM neural network is calculated according to the mean absolute error (MAE), root mean square error (RMSE), and coefficient of determination (R^2).

$$\text{MAE} = \frac{1}{m} \sum_{i=1}^m |y_i - \hat{y}_i|,$$

$$\text{RMSE} = \sqrt{\frac{1}{m} \sum_{i=1}^m (y_i - \hat{y}_i)^2}, \tag{3}$$

$$R^2 = 1 - \frac{\sum_{i=1}^m (y_i - \hat{y}_i)^2}{\sum_{i=1}^m (y_i - \bar{y})^2}.$$

In this paper, a total of two LSTM predictions are made to analyse the influence of the change of air conditioning temperature setting value on the cooling rate, heating rate, and PMV. The input characteristics of the first LSTM do not include the temperature setting value. LSTM trains and predicts the output when the air conditioning temperature setting value is fixed at 26°C. A pseudorandom temperature setpoint between 24°C and 28°C coming from the Simulink block is transferred to EnergyPlus with the same time step. Data are obtained through EnergyPlus simulation and calculated the difference with the result of the first simulation. The second LSTM takes the difference of the temperature setpoints (from -2°C to 2°C) and the prediction results of 26°C as the input characteristics to predict the difference. The final prediction result is obtained by adding and correcting the former prediction results.

The co-simulation model of MATLAB and EnergyPlus obtains the local air dry bulb temperature, relative humidity, solar radiation, and other data from the weather file and transmits them to the LSTM prediction model in EnergyPlus and MATLAB through the BCVTB interface.

2.4. EnergyPlus and Matlab Co-simulation. The calculation process of EnergyPlus is equivalent to a loop in the Matlab program as shown in Figure 3. The condition of the loop is that the simulation time is less than the end time. The content of the loop is to obtain the output of EnergyPlus first and then the input of the BCVTB interface. Therefore, it is necessary to set an initial value of the input. During the

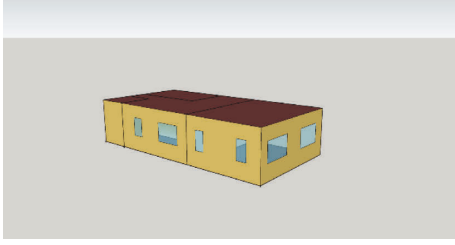


FIGURE 1: EnergyPlus building model in SketchUp.

loop, the inputs will be calculated into outputs in combination with weather data, building structure, and HVAC settings.

In the co-simulation model, k represents the value of the current time, $k + 1$ represents the value of the next time, and the interval between the two values is 10 minutes or 1 hour. The LSTM model obtains the value at time k , predicts the thermal comfort, cooling rate, and heating rate at time $k + 1$, and compares the LSTM predicted value at time $k - 1$ with the actual output value of EnergyPlus at time k . Calculates

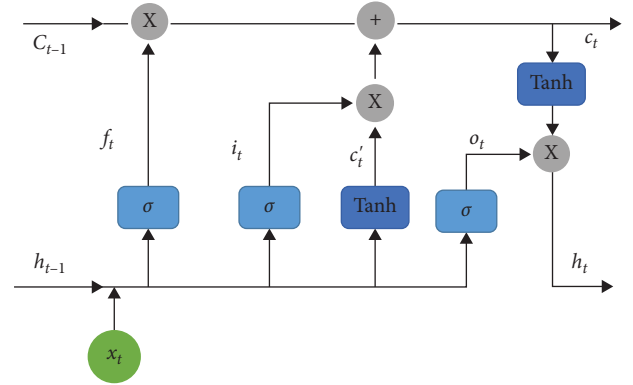


FIGURE 2: Diagram showing the LSTM calculation process.

the error and adds a coefficient as a correction. Based on the predicted value of thermal comfort, using the optimization algorithm, select the appropriate value of air conditioning temperature and input it into EnergyPlus to complete the loop calculation.

$$\begin{aligned}
 y_r(k+i) &= (1 - \alpha^i) y_{sp} + \alpha^i y(k), \\
 e(k) &= y(k) - y_M(k), \\
 y_p(k+i) &= y_M(k+i) + h * e(k), \\
 \min J(k) &= \sum_{i=1}^P q_i [(y_p(k+i) - y_r(k+i))]^2 + \sum_{j=1}^C r_j u^2(k+j-1).
 \end{aligned} \tag{4}$$

In the co-simulation, the optimization condition is the minimum energy consumption of HVAC or the minimum energy consumption under the condition of ensuring thermal comfort. The calculation amount for optimal operation of the HVAC system is increasing, especially if the prediction horizon is extended.

3. Results and Discussion

According to the EnergyPlus weather document, the outdoor temperature in the area changed dramatically from March 1 to April 1. The maximum outdoor temperature is close to 34°C, the minimum temperature is close to 14°C, and the temperature span is nearly 20°C. Single cooling or heating temperature of 26°C will cause unnecessary energy waste. Air conditioning systems with room temperature set to a constant value tend to waste energy unnecessarily during seasonal switching periods. By querying and simulating the outdoor temperature throughout the year, it is found that the outdoor temperature changes drastically in March and April. When the room temperature is set to 26°C, the changes in indoor and

outdoor temperature, cooling power, and heating power are shown in Figure 4.

When the temperature is set to be constant at 26°C, the PMV cooling rate and heating rate at time $k + 1$ are predicted by the LSTM neural network. The input characteristics include PMV, cooling rate, heating rate, outdoor temperature, clothing thermal resistance, occupancy, and outdoor relative humidity at time k .

Pearson correlation coefficient is used to test the correlation extent of the input characteristics of the LSTM prediction. The Pearson correlation coefficients are shown in Figure 5.

Principal component analysis is used to reduce the dimension of the data. According to the principal component analysis, the contribution rates are 48.8087%, 18.2022%, 13.4150%, 7.7321%, 4.4815%, 3.7200%, 2.3225%, 1.0113%, 0.3066%. Therefore, solar radiation is not considered as the input characteristic in this paper.

The prediction results of the back-propagation (BP) neural network and support vector machine (SVM) are used to be compared with the results of LSTM as shown in Tables 3 and 4.

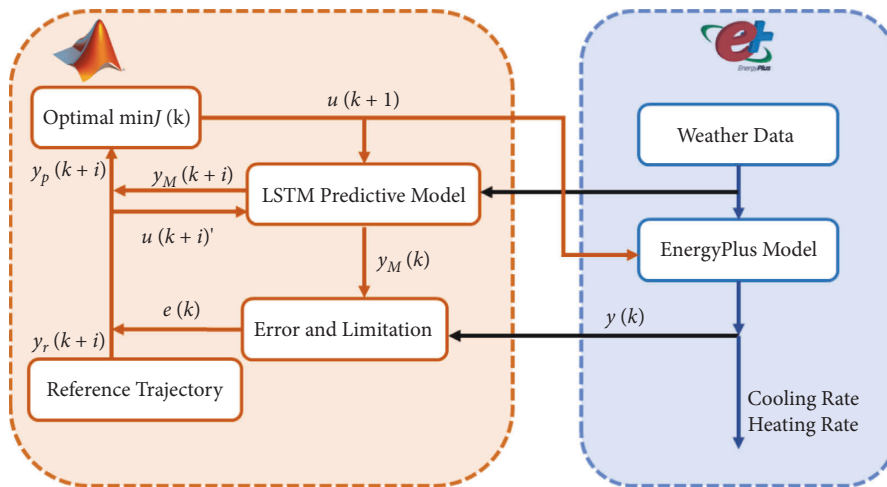


FIGURE 3: Diagram showing EnergyPlus and Matlab cosimulation.

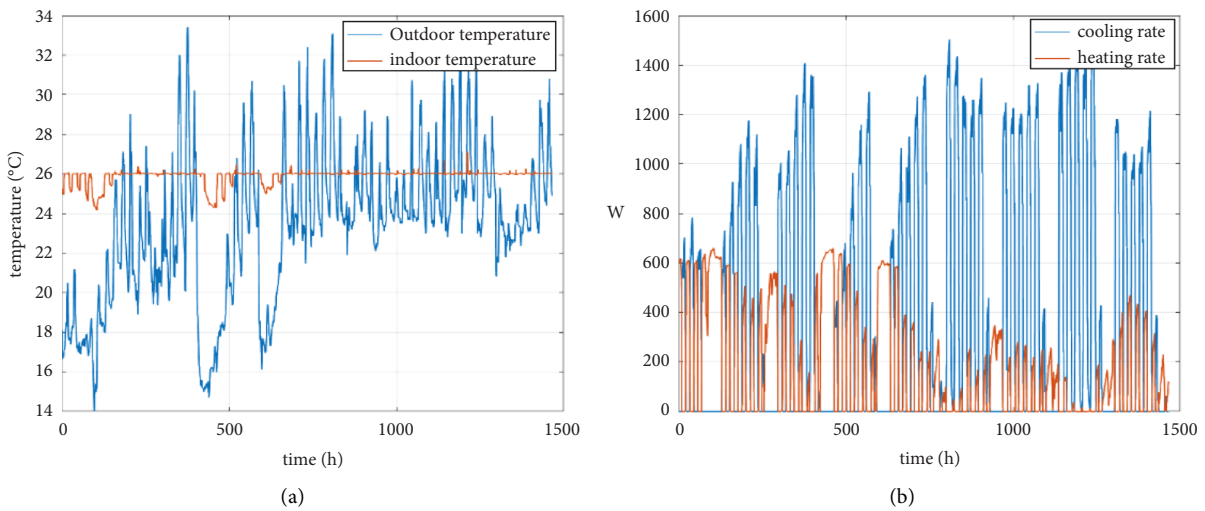


FIGURE 4: (a) The temperature of the zone when the temperature setpoint at 26°C. (b) The cooling and heating rate when temperature setpoints at 26°C.

Cooling Rate	1	-0.5848	0.5403	0.4894	-0.2125	0.9332	-0.3976	0.3916	0.4945
Heating Rate	-0.5848	1	-0.8453	-0.6662	0.5263	-0.6218	0.1607	-0.2292	-0.3159
PMV	0.5403	-0.8453	1	0.7571	-0.5461	0.4954	-0.08616	0.2195	0.2356
Outdoor Temperature	0.4894	-0.6662	0.7571	1	-0.6471	0.3244	-0.4221	0.5048	0.3333
Cloth Value	-0.2125	0.5263	-0.5461	-0.6471	1	-0.08817	0.04499	-0.1111	-0.07249
Occupancy	0.9332	-0.6218	0.4954	0.3244	-0.08817	1	-0.3044	0.2795	0.4552
Outdoor Relative Humidity	-0.3976	0.1607	-0.08616	-0.4221	0.04499	-0.3044	1	-0.5852	-0.4323
Solar Direct Radiation	0.3916	-0.2292	0.2195	0.5048	-0.1111	0.2795	-0.5852	1	0.2198
Solar Diffuse Radiation	0.4945	-0.3159	0.2356	0.3333	-0.07249	0.4552	-0.4323	0.2198	1
	CR	HR	PMV	To	Cloth	Occu	RH	SR1	SR2

FIGURE 5: The Pearson correlation coefficients between the input variables.

TABLE 3: Prediction error of the HVAC system at 26°C.

	MAE	RMSE	R^2
BP: PMV	0.0043	0.0074	0.9891
BP: Cooling rate	42.6323	92.6838	0.9694
BP: Heating rate	6.8774	19.5097	0.9725
SVM: PMV	0.0072	0.0097	0.9827
SVM: Cooling rate	49.0464	99.7086	0.9619
SVM: Heating rate	13.9655	22.6567	0.9558
LSTM: PMV	0.0049	0.008	0.9817
LSTM: Cooling rate	37.2096	88.4511	0.9717
LSTM: Heating rate	8.1833	19.6245	0.9710

TABLE 4: Prediction error of the difference with pseudorandom thermostats.

	MAE	RMSE	R^2
BP: PMV	0.1147	0.1325	-14.1410
BP: Cooling rate	104.5797	164.7057	0.6728
BP: Heating rate	59.4123	86.6870	0.6222
SVM: PMV	0.1144	0.1328	-14.4155
SVM: Cooling rate	164.2922	205.2105	0.1735
SVM: Heating rate	96.1758	125.7699	-1.1372
LSTM: PMV	0.0185	0.0249	0.9648
LSTM: Cooling rate	92.0648	131.9387	0.8092
LSTM: Heating rate	49.9098	69.1809	0.7799

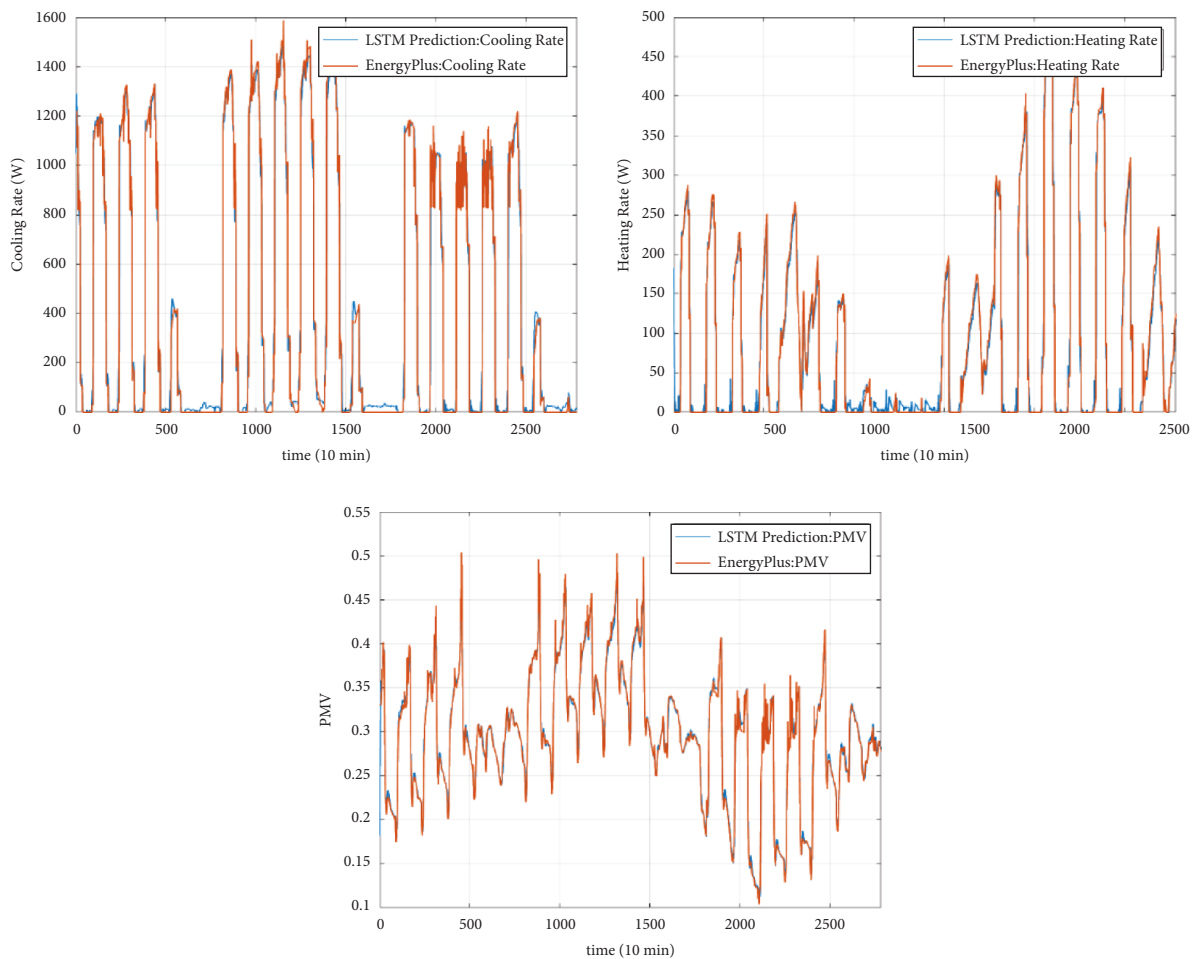


FIGURE 6: The LSTM prediction of the cooling rate, heating rate, PMV at 26°C.

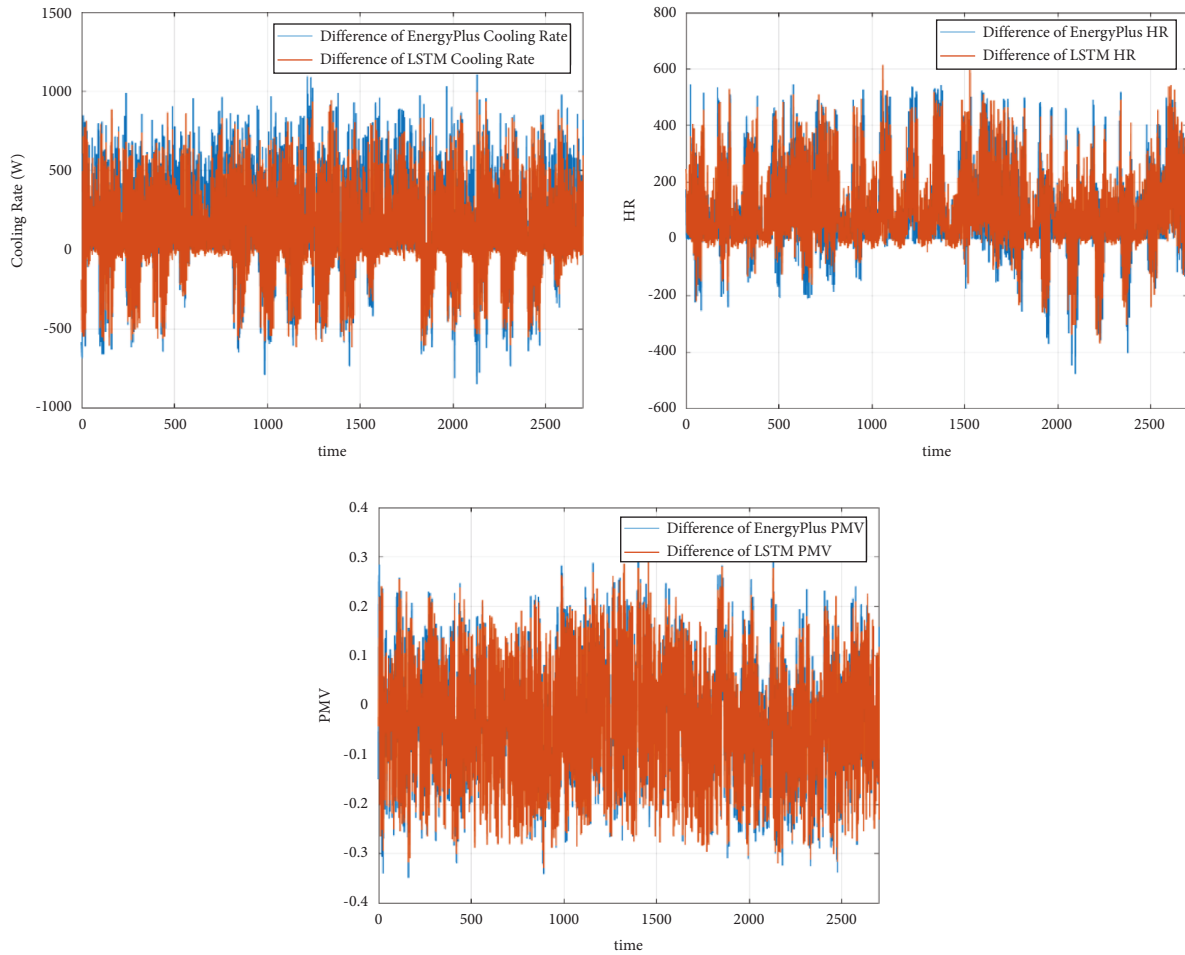


FIGURE 7: The LSTM prediction of the cooling rate difference, heating rate difference, and PMV difference with pseudorandom temperature setpoint.

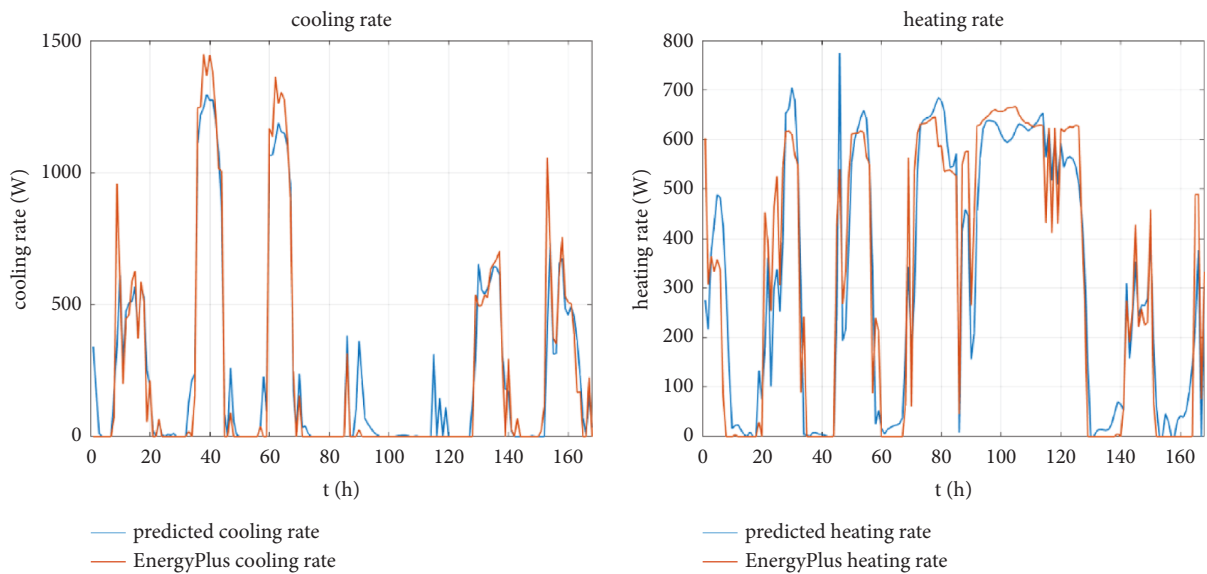


FIGURE 8: The LSTM prediction of heating rate and cooling rate in the cosimulation.

The difference in data compared to 26°C is calculated to clear the relationship between the effect of temperature setpoint changes and the prediction results as shown in

Figures 6 and 7. When the temperature setpoints of the HVAC system change randomly, the accuracy of LSTM prediction is higher than that of SVM and BP.

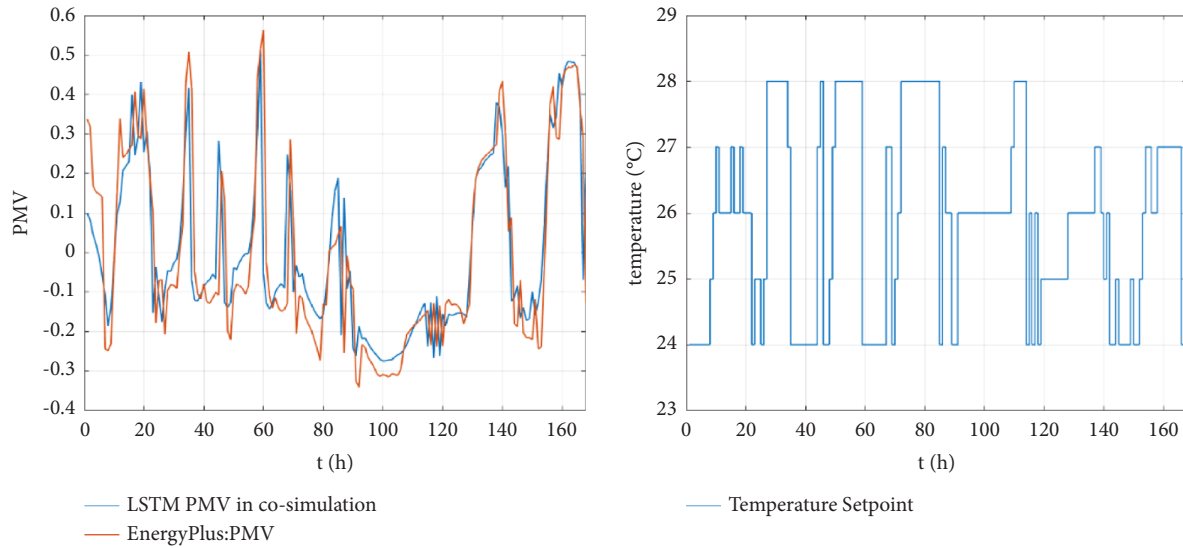


FIGURE 9: The LSTM prediction of PMV in the simulation and the selected temperature.

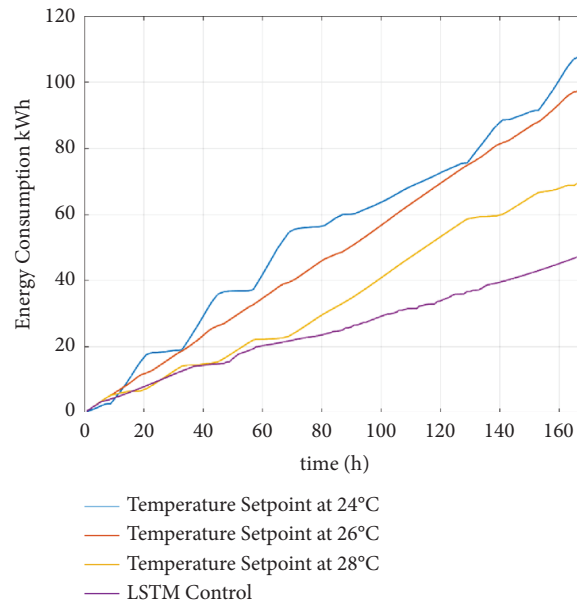


FIGURE 10: The energy consumption with different temperature control methods.

To avoid frequent changes in the temperature setpoint of the HVAC system, the time step of the predictive control in the co-simulation is extended to one hour. The LSTM neural network generated by the prediction of the differences is used to reduce the error. When the optimization condition is the minimum energy consumption of HVAC, the simulation results are shown in Figures 8 and 9.

From the analysis of previous literature and simulation results, the difficulty of thermal comfort prediction mainly is the lack of data. The prediction of air conditioning energy consumption often needs to remove outliers, obtaining parameters of the operating system, such as the temperature or pressure of the refrigerant. Therefore, the accuracy of the prediction has decreased in the real-time control of the co-simulation simulation for various reasons. In Figure 10, the sum of cooling and heating energy consumption with LSTM

predictive control in a week is 47.6903 kWh. When the single cooling or heating setpoint is 26°C, the sum of energy consumption is 98.4682 kWh. The energy consumption is 109.2425 kWh at 24°C and 70.7526 kWh at 28°C.

To meet different application scenarios, different control equations are established. For complex and nonlinear HVAC systems, there are often contradictions between different control conditions. Simulation time changed from July 1st to August 31st, and the training and prediction methods of the LSTM neural network are the same as the previous simulation. If the control conditions are directly set to the minimum value of the energy consumption of the HVAC system that limits the PMV between -0.5 and 0.5 , the indoor temperature will fluctuate. The temperature setpoint needs to avoid frequent changes by setting the softening factor as shown in Figure 11.

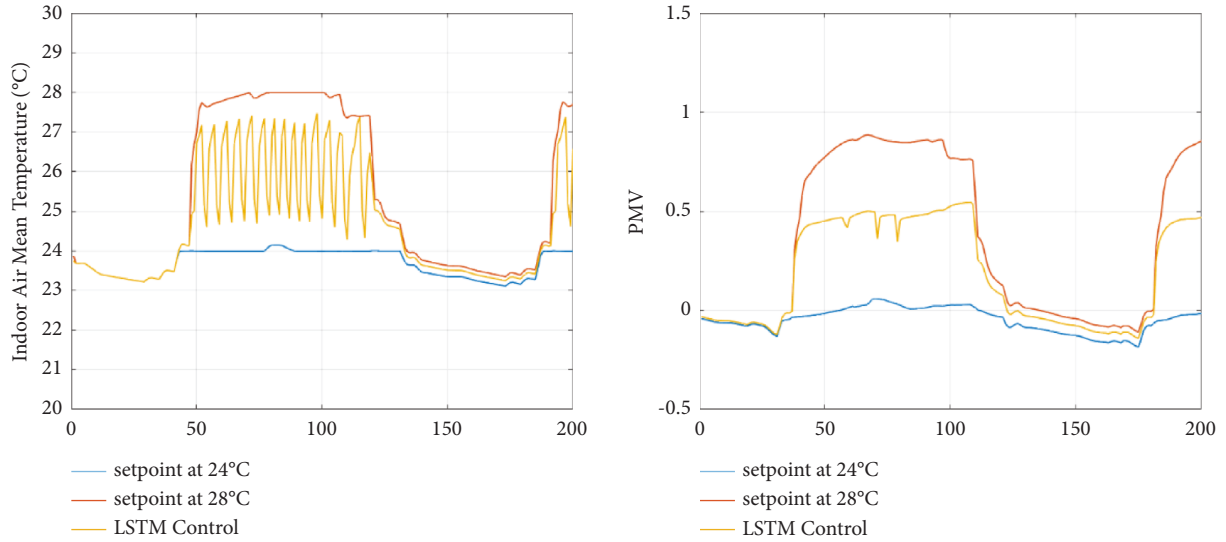


FIGURE 11: The LSTM predictive control with limitation of PMV.

4. Conclusions

In this paper, a Matlab and EnergyPlus co-simulation was established to study the accuracy of LSTM prediction based on weather data and occupancy. EnergyPlus can provide accurate and useful simulation results, while Matlab can provide LSTM prediction and control strategies. The results show that LSTM has stronger antiinterference in the accuracy of prediction. The predictive control supported by LSTM neural network can save 25.70% energy consumption of the HVAC system in a certain seasonal variation period.

There are contradictions in the actual HVAC control of temperature setpoints. For example, the temperature setpoint will always be the maximum value (28°C) when the control condition is only the minimum energy consumption in the simulation from July 1st to August 31st. Energy consumption will be increased when thermal comfort limits are imposed.

LSTM predicted control with a single predictive time step is limited, especially when the outdoor temperature rises rapidly. With the increase of the prediction step, the simulation results will become more stable. The prediction and comparison of different time steps need to be further studied and verified.

Nomenclature

- M : Metabolic rate in PMV calculation (W/m^2)
- W_p : Mechanical work of people in PMV calculation (W/m^2)
- p_a : Air pressure (Pa)
- T_a : Mean air temperature ($^{\circ}C$)
- T_{cl} : Temperature of the cloth surface ($^{\circ}C$)
- T_r : Mean radiant temperature ($^{\circ}C$)
- h_c : Convective heat transfer coefficient ($W/(m^2 \cdot K)$)
- f_{cl} : Clothing area coefficient

- I_{cl} : Clothing isolation ($(m^2 \cdot K)/W$)
- I_{clr} : Relative clothing isolation ($(m^2 \cdot K)/W$)
- v_{ar} : Relative air speed (m/s)
- x : Input of the LSTM
- h : Output of the LSTM
- b : Constant, σ and Tanh denote activation function
- W : Weight coefficient
- m : Number of samples
- \bar{y} : Target mean value
- y_i : Target value
- \hat{y}_i : Output value
- y_r : Expected output
- y_{sp} : Setting value of the system output
- y : Output of the EnergyPlus
- y_M : LSTM neural network and other prediction models replace the system identification model to provide the data
- $e(k)$: The error of the last prediction
- :
- y_p : Correction value of model prediction
- h : The coefficient of the prediction error
- α^i : Softness parameter
- r_j : Weighting coefficient of output
- q_i : Weighting coefficient of input
- P : Prediction horizon
- C : Control horizon.

Data Availability

The datasets used during the study are available from the corresponding author upon reasonable request.

Conflicts of Interest

The authors declare that there are no conflicts of interest with this study.

Acknowledgments

The authors gratefully acknowledge the financial support of National Natural Science Foundation of China (Grant no. 51575286) and Key R&D Plan of Shandong Province (public welfare science and technology research) (Grant no. 2018GGX 105007).

References

- [1] J. Wang, Y. Zhang, and M. Liu, "Comparison of building energy consumption benchmark in China, US and UK," *Building Science*, vol. 31, no. 10, pp. 48–51, 2015.
- [2] A. Lanko, F. J. Sanchez de la Flor, and T. Narezhnaya, "A review on buildings energy consumption in Russia: educational buildings," *E3S Web of Conferences*, vol. 164, no. 11, Article ID 02001, 2020.
- [3] R. Ming, W. Yu, and X. Zhao, "Assessing energy saving potentials of office buildings based on adaptive thermal comfort using a tracking-based method," *Energy and Buildings*, vol. 208, no. Feb, pp. 109611.109611–109611.109614, 2020.
- [4] C. D. Korkas, S. Baldi, I. Michailidis, and E. B. Kosmatopoulos, "Intelligent energy and thermal comfort management in grid-connected microgrids with heterogeneous occupancy schedule," *Applied Energy*, vol. 149, pp. 194–203, 2015.
- [5] R. F. De Masi, A. Gigante, V. Festa, S. Ruggiero, and G. P. Vanoli, "Effect of HVAC's management on indoor thermo-hygrometric comfort and energy balance: in situ assessments on a real nZEB," *Energies*, vol. 14, no. 21, p. 7187, 2021.
- [6] A. Afram and F. Janabi-Sharifi, "Review of modeling methods for HVAC systems," *Applied Thermal Engineering*, vol. 67, no. 1-2, pp. 507–519, 2014.
- [7] A. Afram and F. Janabi-Sharifi, "Theory and applications of HVAC control systems - a review of model predictive control (MPC)," *Building and Environment*, vol. 72, pp. 343–355, 2014.
- [8] M. Soudari, V. Kaparin, S. Srinivasan, S. Seshadhri, and U. Kotta, "Predictive smart thermostat controller for heating, ventilation, and air-conditioning systems," *Proceedings of the Estonian Academy of Sciences*, vol. 67, no. 3, pp. 291–299, 2018.
- [9] J. Ma, J. Qin, T. Salisbury, and P. Xu, "Demand reduction in building energy systems based on economic model predictive control," *Chemical Engineering Science*, vol. 67, no. 1, pp. 92–100, 2012.
- [10] B. Peng and S. J. Hsieh, "Simulation Model of Automated HVAC system control strategy with thermal comfort and occupancy considerations," in *Proceedings of the Asme International Manufacturing Science & Engineering Conference Collocated with the Jsme/asme International Conference on Materials & Processing*, p. V003T004A003p. V003T004A003, 2017.
- [11] C. Lapusan, R. Balan, O. Hancu, and A. Plesa, "Development of a multi-room building thermodynamic model using simscape library," *Energy Procedia*, vol. 85, pp. 320–328, 2016.
- [12] K. Venkatesan and U. Ramachandriah, "Climate responsive cooling control using artificial neural networks," *Journal of Building Engineering*, vol. 19, pp. 191–204, 2018.
- [13] N. Alibabaei, A. S. Fung, and K. Raahemifar, "Development of Matlab-TRNSYS co-simulator for applying predictive strategy planning models on residential house HVAC system," *Energy and Buildings*, vol. 128, pp. 81–98, 2016.
- [14] M. Narayanan, A. F. de Lima, A. F. O. de Azevedo Dantas, and W. Commerell, "Development of a Coupled TRNSYS-MATLAB Simulation framework for model predictive control of integrated electrical and thermal residential renewable energy system," *Energies*, vol. 13, no. 21, p. 5761, 2020.
- [15] Y. Wang, K. Velswamy, and B. Huang, "A long-short term memory recurrent neural network based reinforcement learning controller for office heating ventilation and air conditioning systems," *Processes*, vol. 5, no. 3, p. 46, 2017.
- [16] A. Rosato, F. Guarino, S. Sibilio, E. Entchev, M. Masullo, and L. Maffei, "Healthy and faulty experimental performance of a typical HVAC system under Italian climatic conditions: artificial neural network-based model and fault impact assessment," *Energies*, vol. 14, no. 17, p. 5362, 2021.
- [17] R. Z. Homod, A. Almusaed, A. Almssad, M. K. Jaafar, M. Goodarzi, and K. S. Sahari, "Effect of different building envelope materials on thermal comfort and air-conditioning energy savings: a case study in Basra city, Iraq," *Journal of Energy Storage*, vol. 34, Article ID 101975, 2021.
- [18] X. Y. Lin, H. Yu, M. Wang, C. Li, Z. Wang, and Y. Tang, "Electricity consumption forecast of high-rise office buildings based on the long short-term memory method," *Energies*, vol. 14, no. 16, p. 4785, 2021.
- [19] R. Sendra-Arranz and A. Gutierrez, "A long short-term memory artificial neural network to predict daily HVAC consumption in buildings," *Energy and Buildings*, vol. 216, Article ID 109952, 2020.
- [20] F. Mtibaa, K. K. Nguyen, M. Azam, A. Papachristou, J. S. Venne, and M. Cheriet, "LSTM-based indoor air temperature prediction framework for HVAC systems in smart buildings," *Neural Computing & Applications*, vol. 32, no. 23, pp. 17569–17585, 2020.
- [21] K. F. Huang, K. P. Hallinan, R. B. Lou, A. Alanezi, S. Alshatshati, and Q. Sun, "Self-learning algorithm to predict indoor temperature and cooling demand from smart WiFi thermostat in a residential building," *Sustainability*, vol. 12, no. 17, p. 7110, 2020.
- [22] S. Baldi, C. D. Korkas, M. L. Lv, and E. B. Kosmatopoulos, "Automating occupant-building interaction via smart zoning of thermostatic loads: a switched self-tuning approach," *Applied Energy*, vol. 231, pp. 1246–1258, 2018.
- [23] R. de Dear, J. Xiong, J. Kim, and B. Cao, "A review of adaptive thermal comfort research since 1998," *Energy and Buildings*, vol. 214, Article ID 109893, 2020.
- [24] F. d'Ambrosio Alfano, B. W. Olesen, B. I. Palella, D. Pepe, and G. Riccio, "Fifty Years of PMV model: reliability, implementation and design of software for its calculation," *Atmosphere*, vol. 11, no. 1, p. 49, 2019.
- [25] S. H. Cao, X. Li, B. Yang, and F. Li, "A review of research on dynamic thermal comfort," *Building Service Engineering Research and Technology*, vol. 42, no. 4, pp. 435–448, 2021.
- [26] N. Somu, A. Sriram, and A. Kowli, "A hybrid deep transfer learning strategy for thermal comfort prediction in buildings," *Building and Environment*, vol. 204, 2021.
- [27] C. D. Korkas, S. Baldi, I. Michailidis, and E. B. Kosmatopoulos, "Occupancy-based demand response and thermal comfort optimization in microgrids with renewable energy sources and energy storage," *Applied Energy*, vol. 163, pp. 93–104, 2016.
- [28] B. W. Olesen and K. C. Parsons, "Introduction to thermal comfort standards and to the proposed new version of EN ISO 7730," *Energy and Buildings*, vol. 34, no. 6, pp. 537–548, 2002.
- [29] S. Hochreiter and J. Schmidhuber, "Long short-term memory," *Neural Computation*, vol. 9, no. 8, pp. 1735–1780, 1997.